

# X-ray absorption spectroscopy as a structural probe of dynamics in fuel cell and battery systems

Carlo Segre

Physics Department  
&  
Center for Synchrotron Radiation Research and Instrumentation  
Illinois Institute of Technology

September 28, 2017

# What's a physicist doing speaking at an analytical chemistry seminar?

Carlo Segre

Physics Department  
&  
Center for Synchrotron Radiation Research and Instrumentation  
Illinois Institute of Technology

September 28, 2017



- Introduction to CSRRRI & MRCAT
- X-ray absorption spectroscopy
- Operando synchrotron fuel cells
- Methanol oxidation on a PtRu catalyst
- Ru@Pt core-shell methanol catalysts
- Sn anodes for Li-ion batteries
- Accelerated capacity fading studies
- “Reversible”  $\text{Sn}_4\text{P}_3$ /graphite composite anode



## Tenure-Track Faculty

Carlo Segre	–	Physics
Grant Bunker	–	Physics
Jeff Terry	–	Physics
David Gidalevitz	–	Physics
Tom Irving	–	Biology
Andy Howard	–	Biology
Joseph Orgel	–	Biology
Adam Hock	–	Chemistry

## Beamline Staff

John Katsoudas	–	MRCAT
Al Kwiatkowski	–	MRCAT
Bill Lavender	–	MRCAT
Weikang Ma	–	BioCAT
Carrie Clark	–	BioCAT
Rick Heurich	–	BioCAT
Mark Vukonich	–	BioCAT
Zou Finfrock	–	CLS@APS
Matt Ward	–	CLS@APS

## Research Faculty

Jim Kaduk	–	Chemistry	Bhoopesh Mishra	–	Physics
Elena Timofeeva	–	Chemistry	Joshua Wright	–	Physics
Srinivas Chakravarthy	–	Biology	Ali Khounsary	–	Physics
Elizabeth Friedman	–	CoS	Derrick Mancini	–	Physics
			Bernhard Adams	–	Physics





- 1993 – MRCAT started with materials physics focus  
Notre Dame, Northwestern, Purdue, IIT, Amoco
- 1995 – Construction begins on Insertion Device line  
Univ. of Florida, Argonne/CSE joins
- 1997 – First light on Insertion Device line
- 1998 – Argonne/ER joins
- 2002 – Honeywell, Sandia fund initial Bending Magnet line
- 2005 – EPA joins
- 2007 – UOP joins Bending Magnet line buildout begins
- 2009 – Bending Magnet line operational



## Current active membership

University of Notre Dame

Illinois Institute of Technology

Argonne Chemical Sci. & Eng.

Argonne Biosciences

Environmental Protection Agency

UOP Honeywell

BP p.l.c.



## ID Line

XAFS (4 keV - 65 keV)

Continuous scan (< 2 min)

Very dilute samples

Microprobe

Microdiffraction

HAXPES

## BM Line

XAFS (4 keV - 32 keV)

Continuous scan (~ 4 min)

SDD for dilute samples

Instrumentation

## General users – catalysis

UC Davis, Purdue, Penn State

Illinois, Princeton, UCSB

Rice, LSU, UC Berkeley, Michigan

Wisconsin, Ohio State, MIT, ORNL

NREL, WPAFB, Chicago,

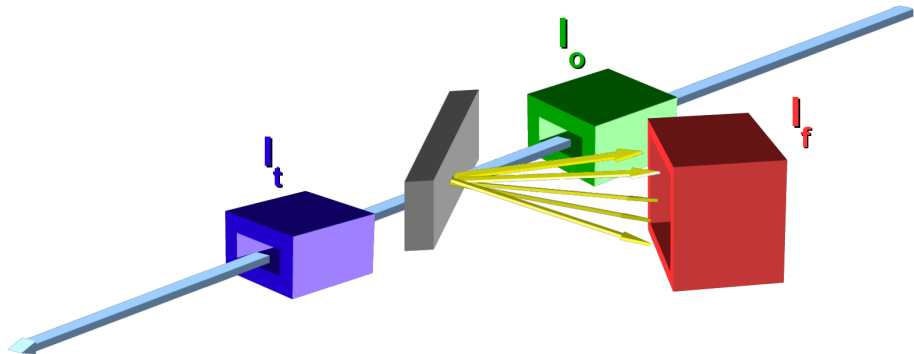
LANL, ...

# The EXAFS experiment



$I_o$  = incident intensity  
 $I_t$  = transmitted intensity  
 $I_f$  = fluorescence intensity

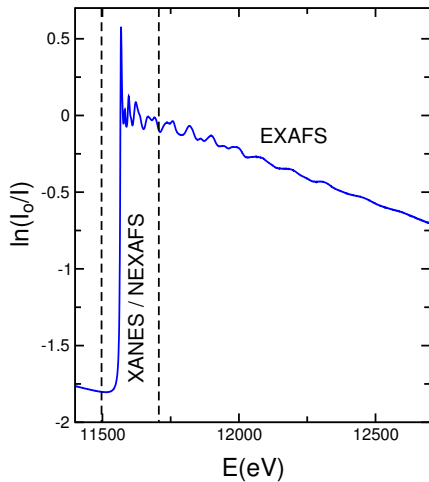
$x$  = sample thickness  
 $\mu(E)$  = absorption coefficient

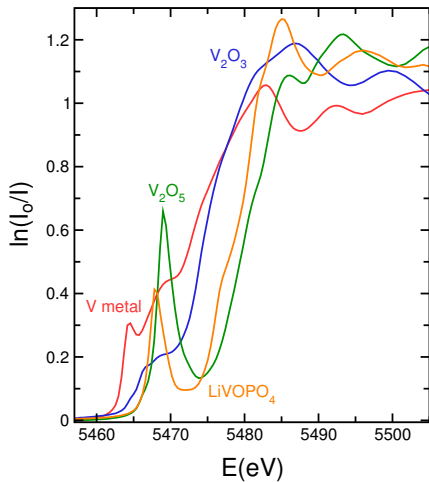
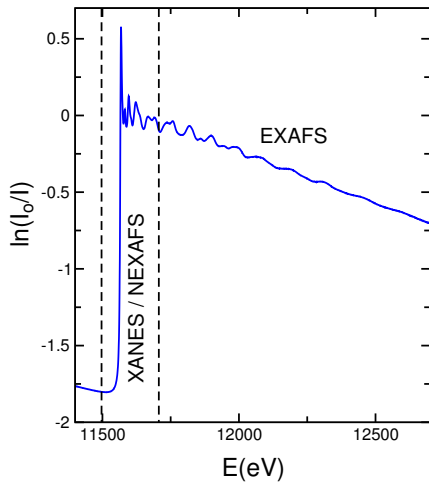


$$I_t = I_o e^{-\mu(E)x}$$

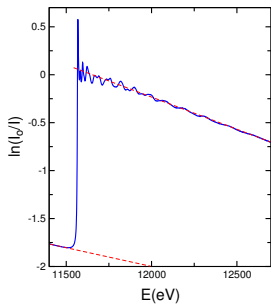
$$\mu(E)x = \ln \left( \frac{I_o}{I_t} \right)$$

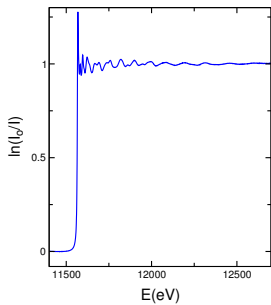
$$\mu(E) \propto \frac{I_f}{I_o}$$

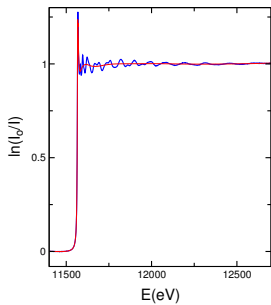




# EXAFS analysis

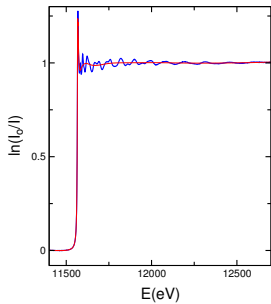




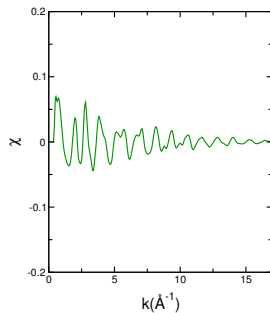




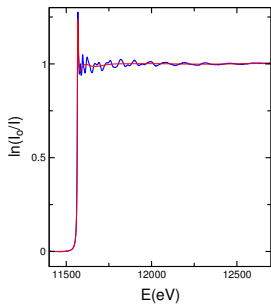
# EXAFS analysis



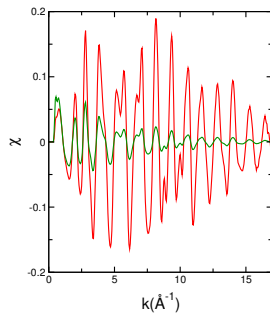
remove background



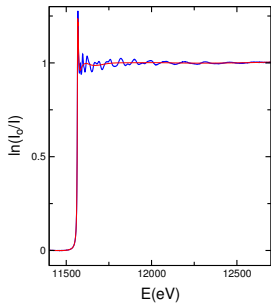
# EXAFS analysis



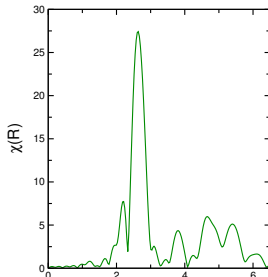
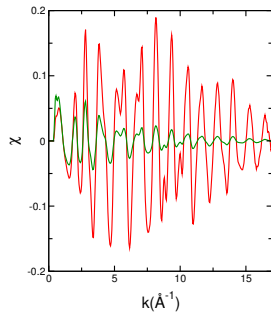
remove background and  
apply k-weighting



# EXAFS analysis

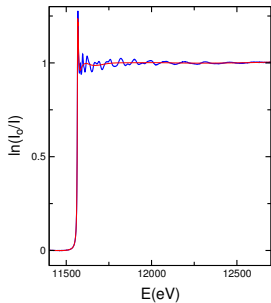


remove background and  
apply k-weighting

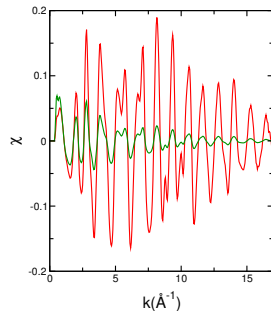


take Fourier Transform

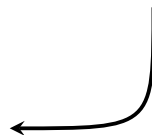
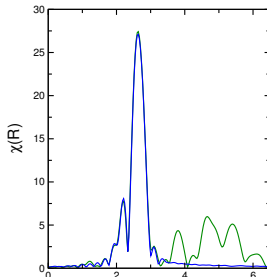
# EXAFS analysis



remove background and  
apply k-weighting

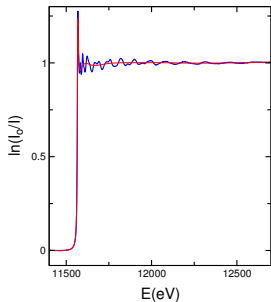


extract structural pa-  
rameters for **first shell**

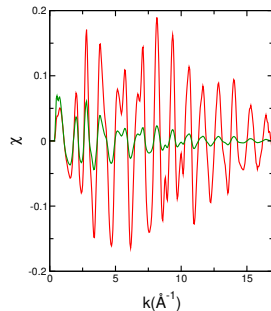


take **Fourier Transform**  
and fit with a structural  
model

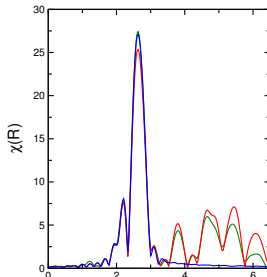
# EXAFS analysis



remove background and  
apply k-weighting

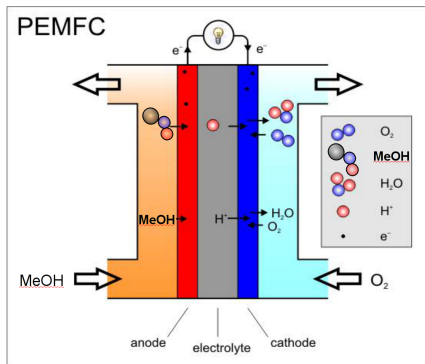


extract structural parameters for **first shell** or **more distant atoms** as appropriate

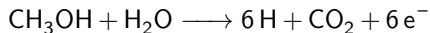


take **Fourier Transform**  
and fit with a structural  
model

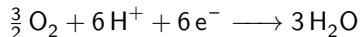
# Methanol oxidation by a PtRu anode



Anode: 0.02 V vs. SHE



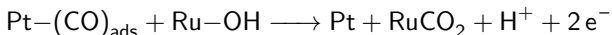
Cathode: 1.23 V s. SHE



Pt surface poisoned by CO

U.S. Department of Defense (DoD) Fuel Cell  
Test and Evaluation Center (FCTec)

The presence of Ru promotes CO oxidation through a  
“bi-functional mechanism”

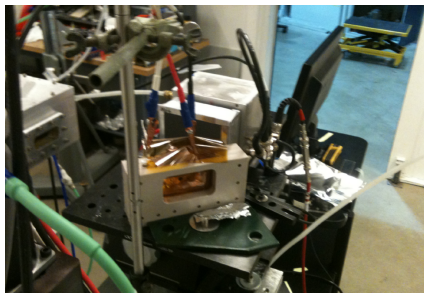
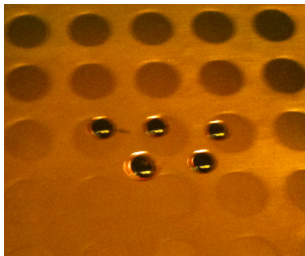
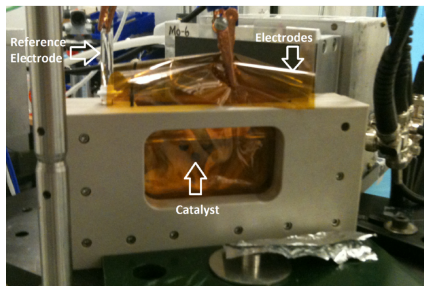
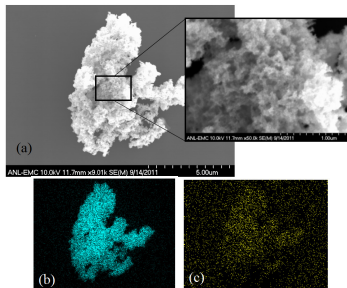




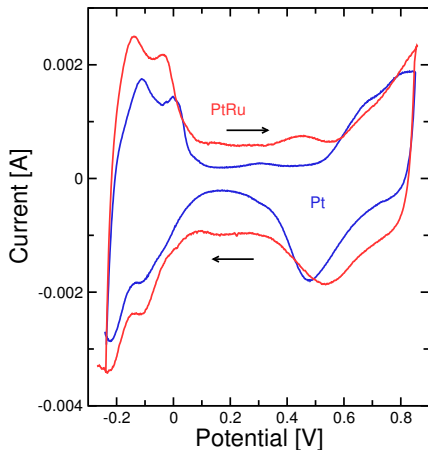
- PtRu bifunctional catalyst improves performance
- In commercial PtRu catalysts there is always a lot of inactive Ru-oxide (?)
- Ru signal dominated by metallic Ru environment
- How does Ru behave in the presence of reactants adsorbed on platinum surface?

Core-shell nanoparticles can resolve these questions

# Ru-decorated Pt nanoparticles





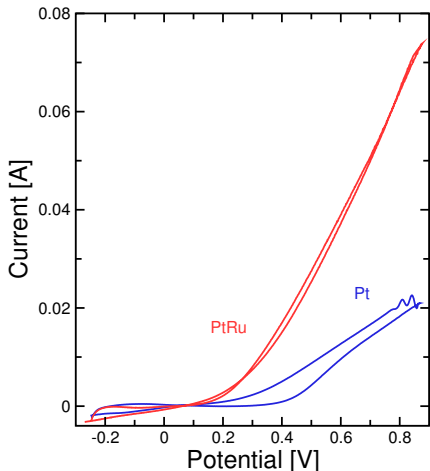


Without Methanol

Low V peaks are  $\text{H}^+$  stripping

Dip at  $\sim 0.5$  V is oxygen stripping

Ru shifts potential on all peaks



Without Methanol

Low V peaks are  $H^+$  stripping

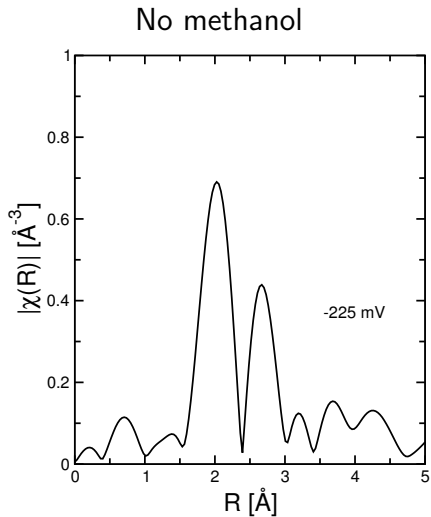
Dip at  $\sim 0.5$  V is oxygen stripping

Ru shifts potential on all peaks

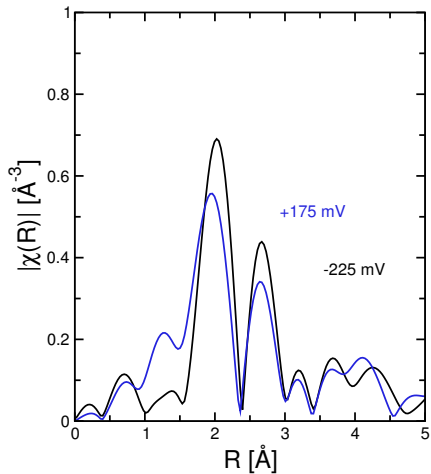
With Methanol

Continual current growth is due to methanol oxidation

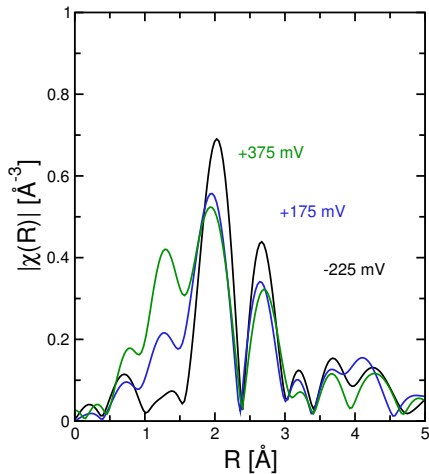
Ru improves current by removing the CO which blocks active sites



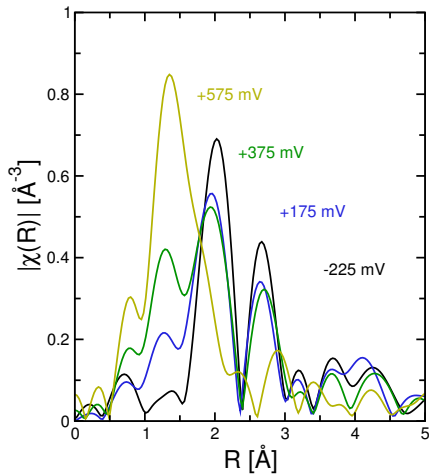
No methanol



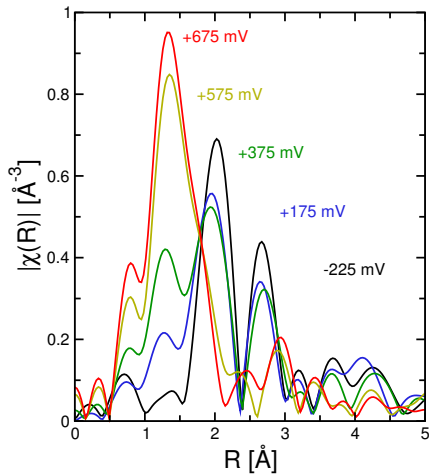
No methanol



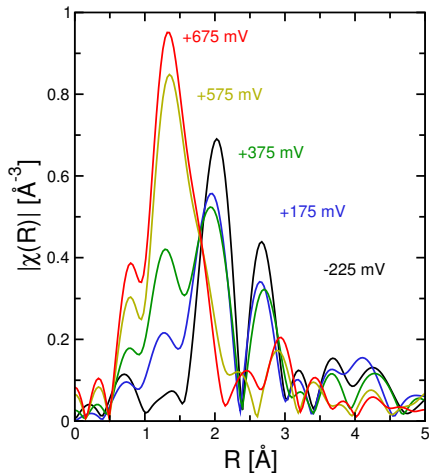
No methanol



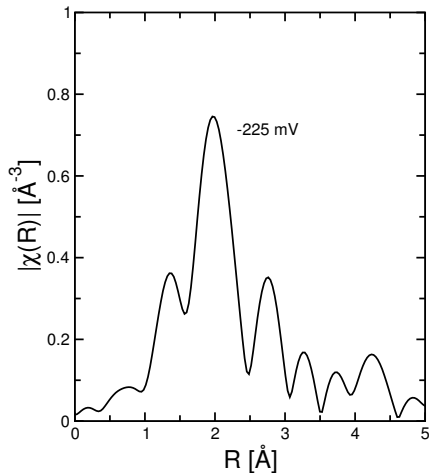
No methanol



No methanol

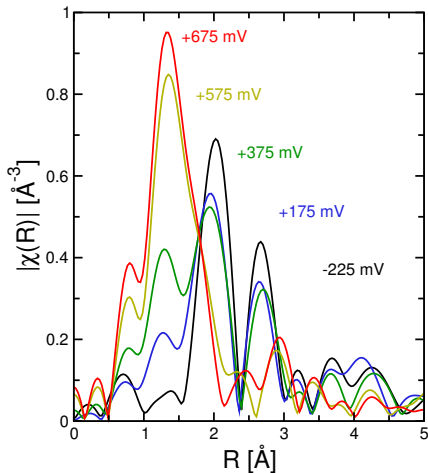


With methanol

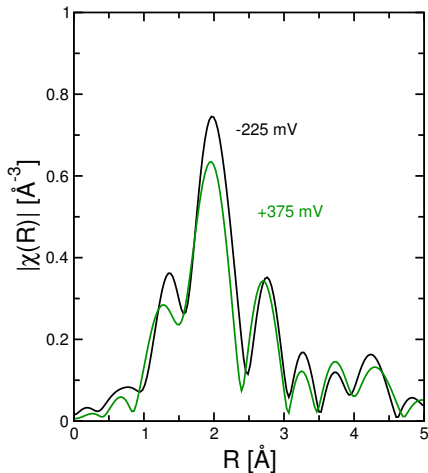




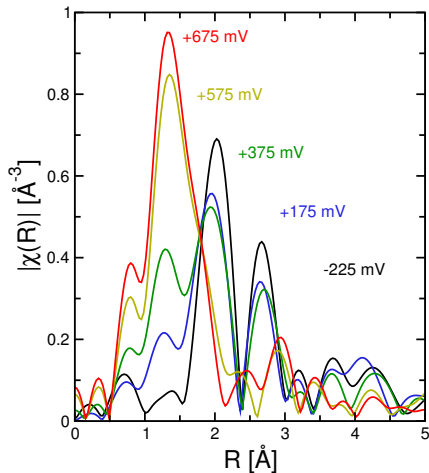
No methanol



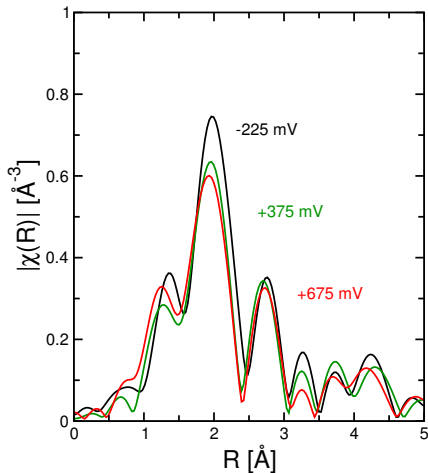
With methanol



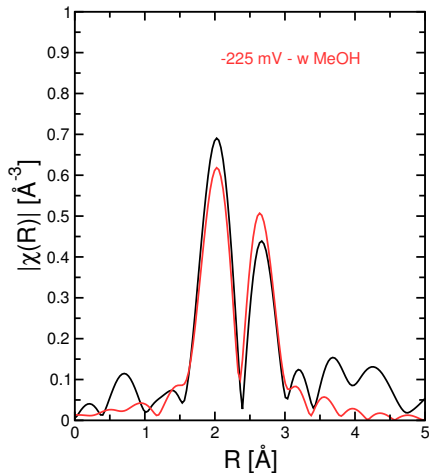
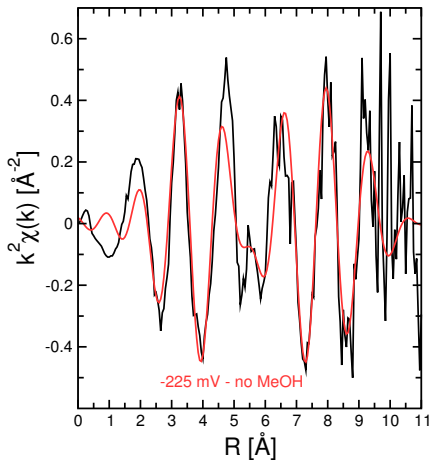
No methanol



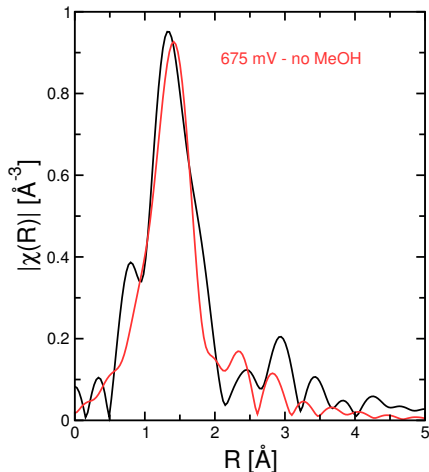
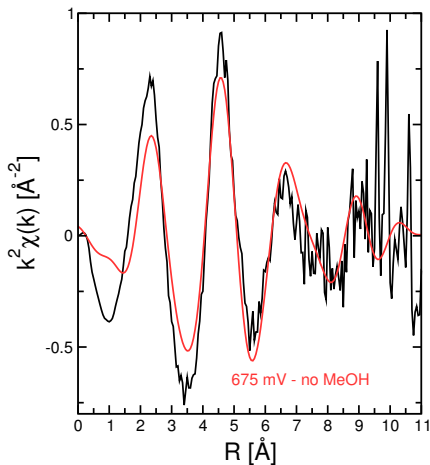
With methanol



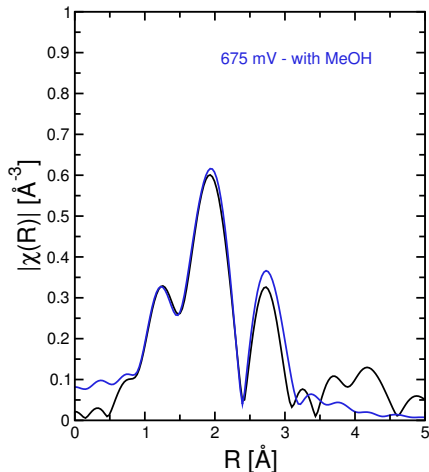
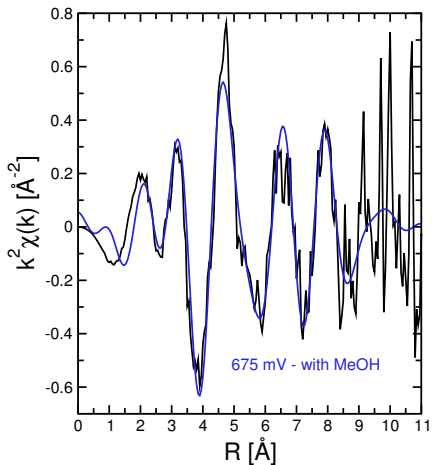
# Fit example: -225 mV without methanol

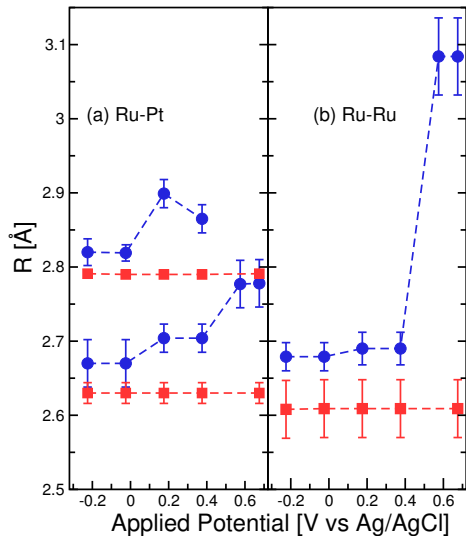


# Fit example: 675 mV without methanol



# Fit example: 675 mV with methanol



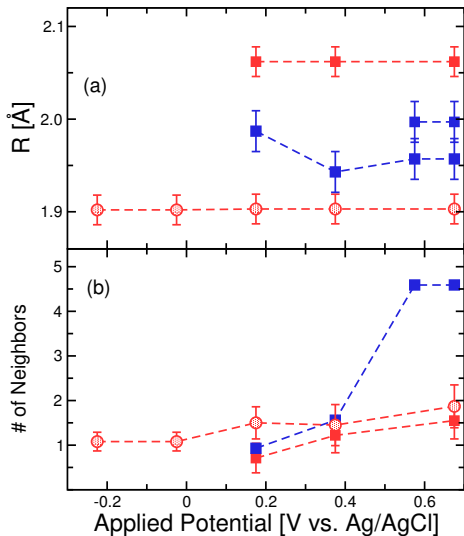


Without methanol

Ru-M distances are longer and  $\text{RuO}_2$  is formed at high potentials

With methanol

Ru-M distances are shorter and remain the same at all potentials

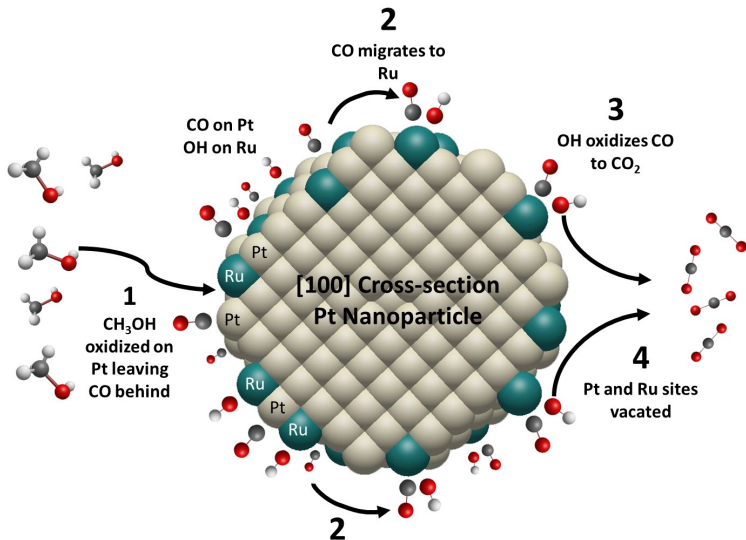


## Without methanol

Above 375 mV Ru-O paths appear and total number of Ru-O neighbors increases to that of RuO<sub>2</sub>

## With methanol

Ru has one low Z neighbor at all potentials (carbon); a second above 175 mV (oxygen) with constant bond lengths and slightly increasing numbers



C. Pelliccione et al., "In situ Ru K-Edge x-ray absorption spectroscopy study of methanol oxidation mechanisms on model submonolayer Ru on Pt nanoparticle electrocatalyst" *J. Phys. Chem. C* **117**, 18904 (2013).





## Cathode materials:

- $\text{Ni}(\text{OH})_2 @ \text{Co}(\text{OH})_2$
- $\text{MnO}_2$
- $\text{LiCoO}_2$
- $\text{Li}_{1.2}(\text{NiMnCo})_{0.8}\text{O}_2$
- $\text{Li}_{1.2}(\text{MnNiFe})_{0.8}\text{O}_2$
- $\text{Li}_3\text{V}_2(\text{PO}_4)_3$
- $\text{LiFePO}_4$

Edge	Energy
Li	0.055 keV
V	5.465 keV
Mn	6.539 keV
Fe	7.112 keV
Co	7.709 keV
Ni	8.333 keV

Li edge not directly accessible and 3d element energies challenging for *in situ* experiments.

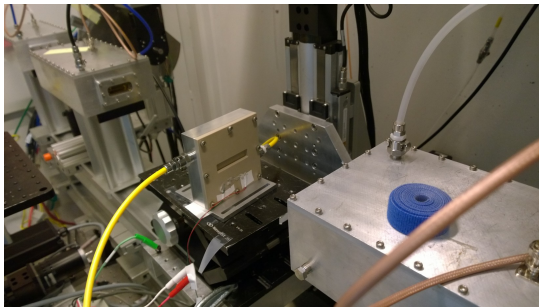
## Anode materials:

- $\text{Fe}_2\text{O}_3$
- $\text{ZnO}$
- $\text{MoS}_2$
- $\text{Sn}$
- $\text{SnO}_2$
- $\text{Sn}_3\text{O}_2(\text{OH})_2$
- $\text{Sn}_4\text{P}_3$

Edge	Energy
P	2.145 keV
S	2.472 keV
Fe	7.112 keV
Zn	9.659 keV
Mo	20.00 keV
Sn	29.20 keV

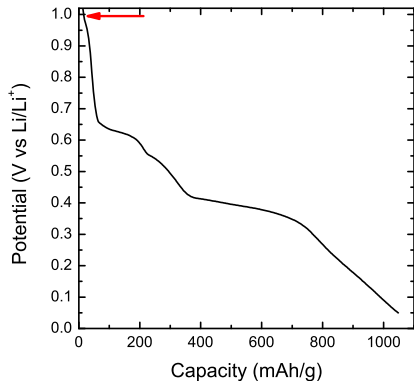
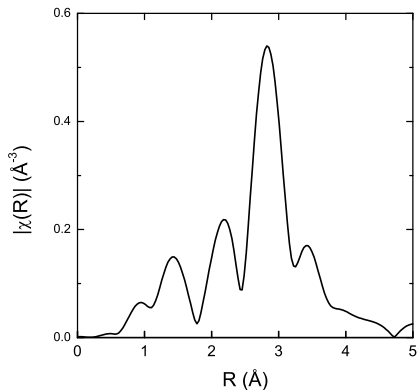
P and S edges too low for non-vacuum experiments, Zn good in fluorescence, Mo and Sn ideal for *in situ* experiments.

- In situ box for non-aqueous experiments
- Have measured  $\text{Sn}_3\text{O}_2(\text{OH})_2$ ,  $\text{SnO}_2$ ,  $\text{Sn}$ ,  $\text{ZnO}$ ,  $\text{MoO}_2$  ...
- Pouch cell simplifies experiment



- MRCAT 10-ID beam line scans EXAFS spectrum in 2 minutes
- Focus on Sn nanoparticles which have rapid failure rate
- Successfully modeled Sn-Li paths in  $\text{Sn}_3\text{O}_2(\text{OH})_2$  using 3 composite paths

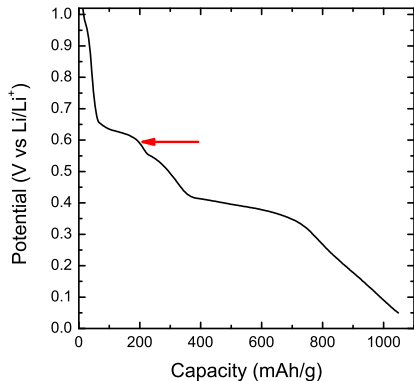
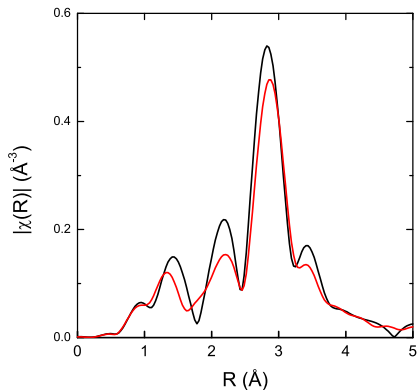
# Sn EXAFS versus potential



$\text{Li}_{22}\text{Sn}_5$  has 14 Sn-Li paths with distance 3.4  $\text{\AA}$  or less

These are modeled using three Sn-Li paths at “center of mass” location

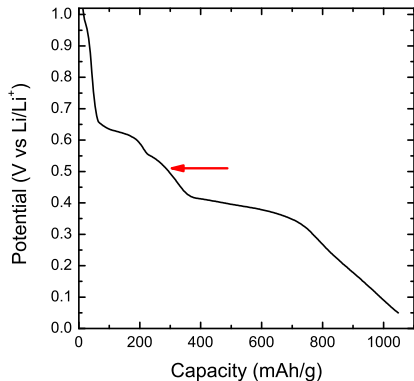
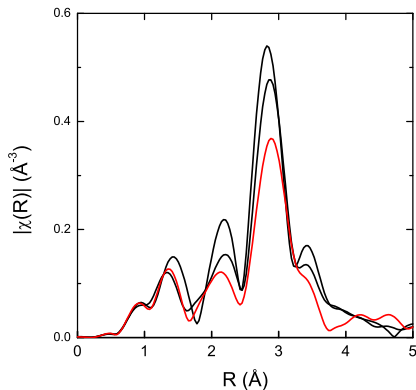
# Sn EXAFS versus potential



$\text{Li}_{22}\text{Sn}_5$  has 14 Sn-Li paths with distance  $3.4 \text{ \AA}$  or less

These are modeled using three Sn-Li paths at “center of mass” location

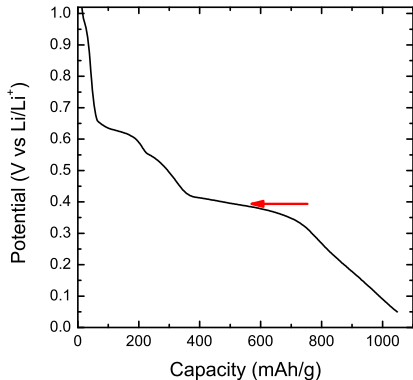
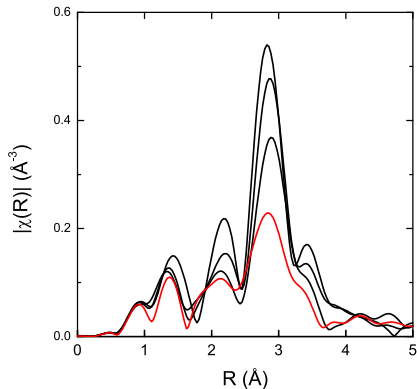
# Sn EXAFS versus potential



$\text{Li}_{22}\text{Sn}_5$  has 14 Sn-Li paths with distance  $3.4 \text{ \AA}$  or less

These are modeled using three Sn-Li paths at “center of mass” location

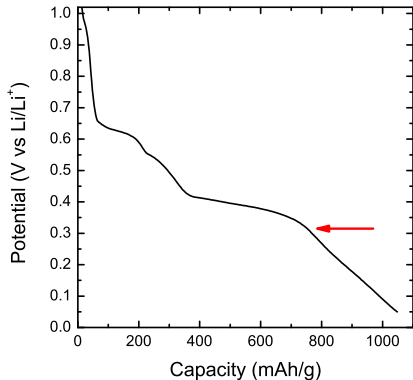
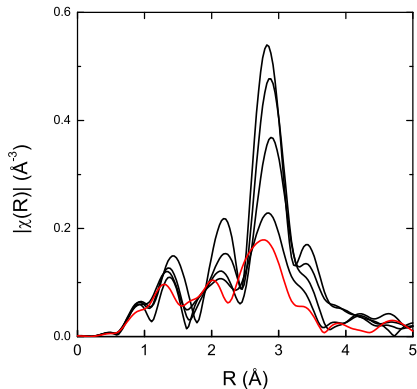
# Sn EXAFS versus potential



$\text{Li}_{22}\text{Sn}_5$  has 14 Sn-Li paths with distance 3.4 Å or less

These are modeled using three Sn-Li paths at “center of mass” location

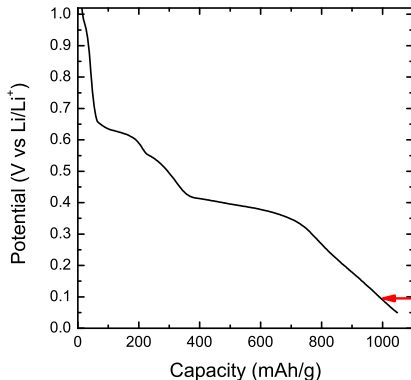
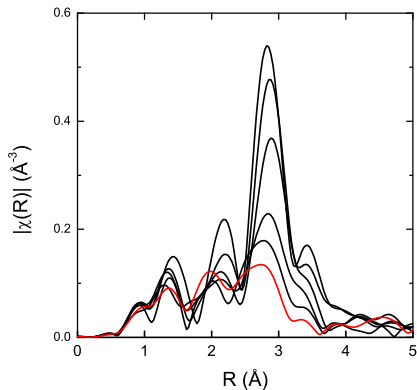
# Sn EXAFS versus potential



$\text{Li}_{22}\text{Sn}_5$  has 14 Sn-Li paths with distance  $3.4 \text{\AA}$  or less

These are modeled using three Sn-Li paths at “center of mass” location

# Sn EXAFS versus potential

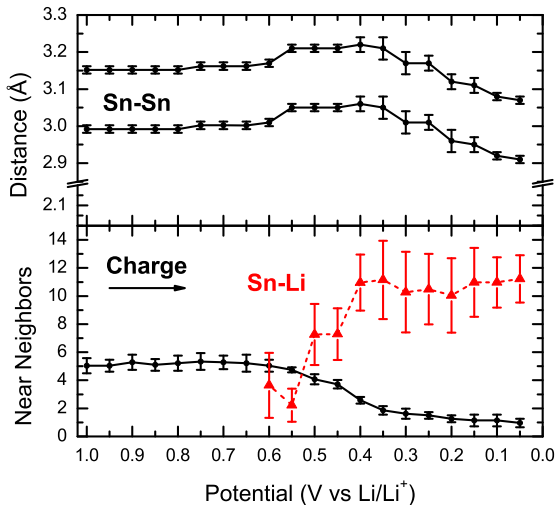


$\text{Li}_{22}\text{Sn}_5$  has 14 Sn-Li paths with distance  $3.4 \text{ \AA}$  or less

These are modeled using three Sn-Li paths at “center of mass” location



# The Sn lithiation process

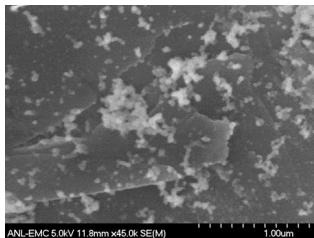


**0.60V** – Sn metal begins to break down and Li appears

**0.45V** – number of Li reaches 11 and stabilizes at near full  $\text{Li}_{22}\text{Sn}_5$

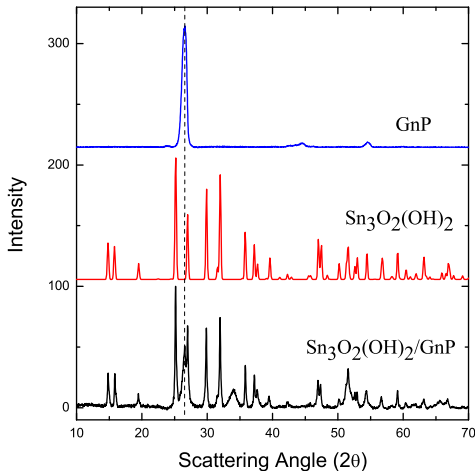
However, Sn fades rapidly due to electric conductivity loss. What can be improved?

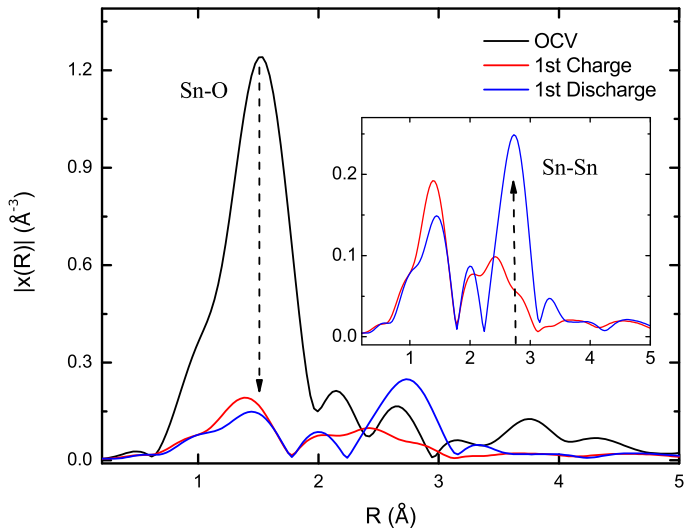
# Synthesis of Sn-graphite nanocomposites

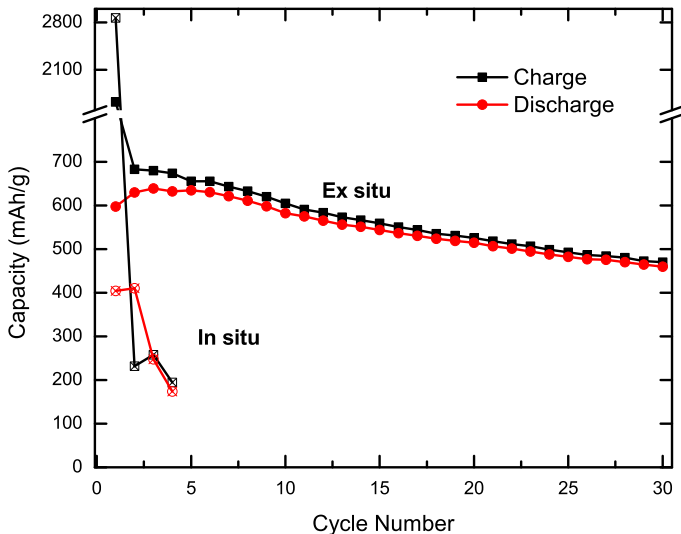


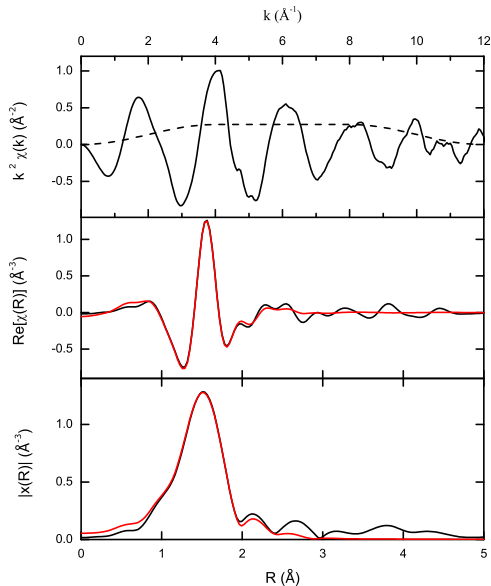
One-pot synthesis produces evenly distributed  $\text{Sn}_3\text{O}_2(\text{OH})_2$  nanoparticles on graphite nanoplatelets

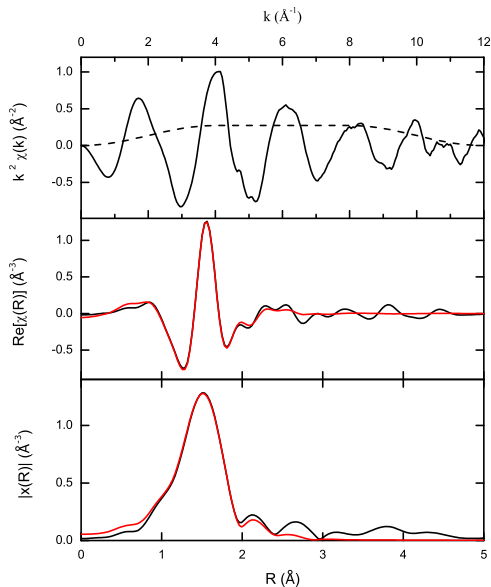
XRD shows a small amount of Sn metal in addition to  $\text{Sn}_3\text{O}_2(\text{OH})_2$



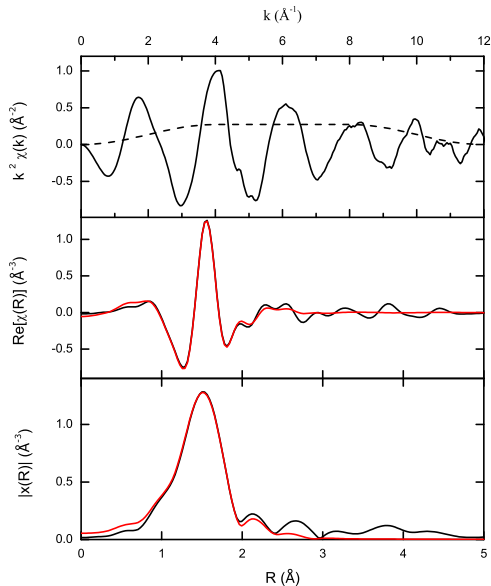






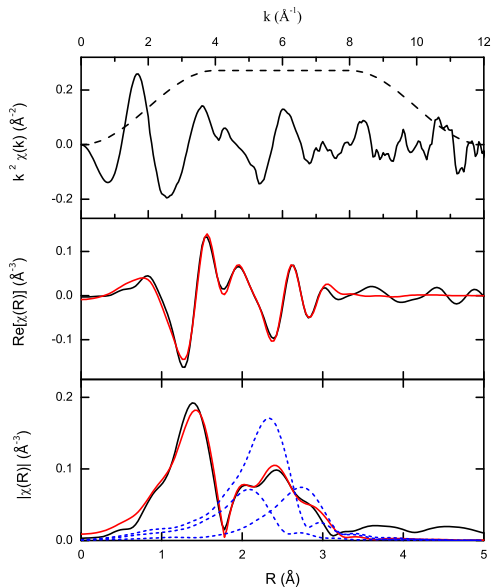


Fresh electrode can be fit with  $\text{Sn}_3\text{O}_2(\text{OH})_2$  structure which is dominated by the near neighbor Sn-O distances



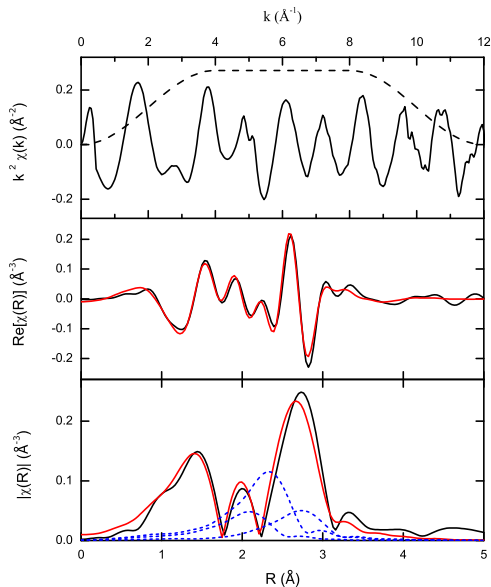
Fresh electrode can be fit with  $\text{Sn}_3\text{O}_2(\text{OH})_2$  structure which is dominated by the near neighbor Sn-O distances

Only a small amount of metallic Sn-Sn distances can be seen

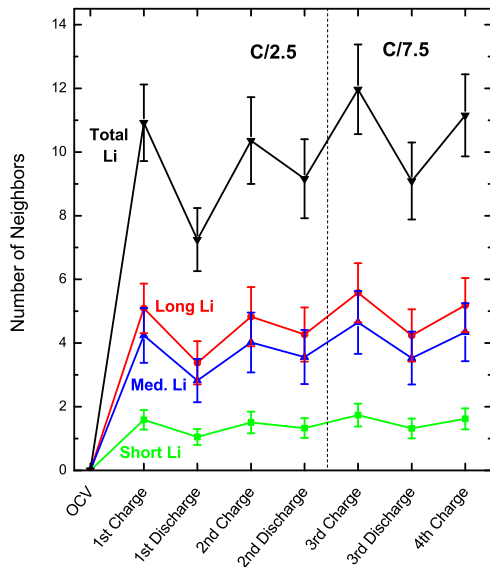


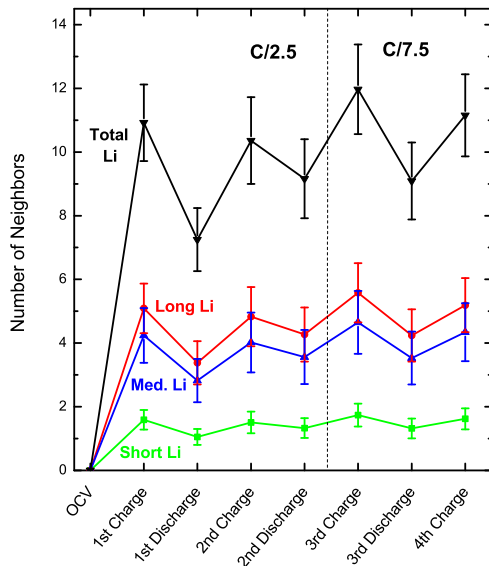
Reduction of number of Sn-O near neighbors and 3 Sn-Li paths characteristic of the  $\text{Li}_{22}\text{Sn}_5$  structure



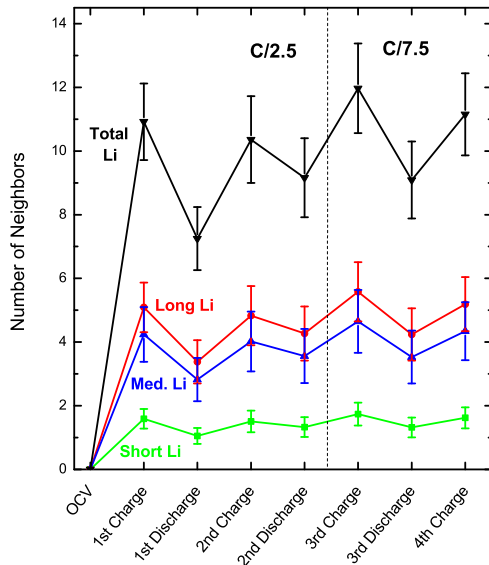


Metallic Sn-Sn distances appear but Sn-Li paths are still present, further reduction in Sn-O near neighbors.



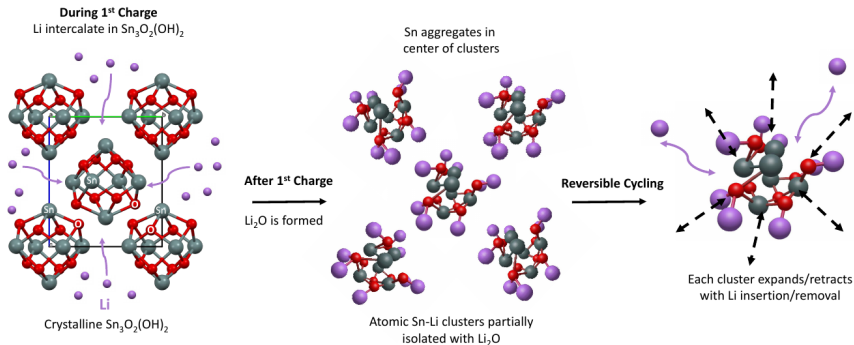


Number of Li near neighbors oscillates with the charge/discharge cycles but never returns to zero



Number of Li near neighbors oscillates with the charge/discharge cycles but never returns to zero

*In situ* cell promotes accelerated aging because of Sn swelling and the reduced pressure of the thin PEEK pouch cell assembly



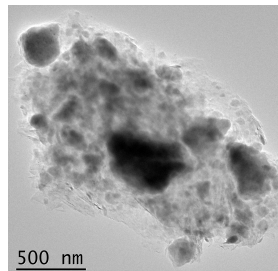
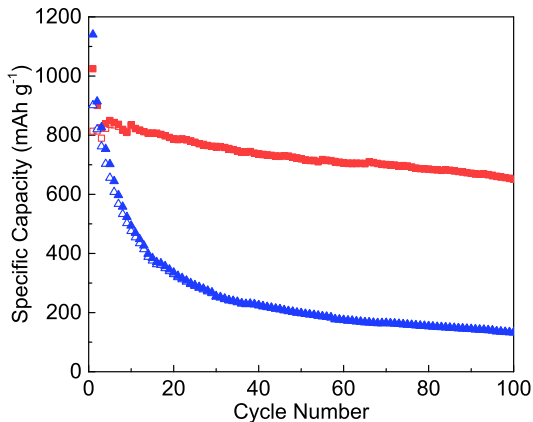
C. Pelliccione et al., "In situ XAS study of the capacity fading mechanism in hybrid  $\text{Sn}_3\text{O}_2(\text{OH})_2$ /graphite battery anode nanomaterials", *Chem. Mater.* 27, 574-580 (2015).

# Sn<sub>4</sub>P<sub>3</sub>/graphite composite anode



Sn<sub>4</sub>P<sub>3</sub> synthesized by high energy ball milling, then ball milled again with graphite to obtain composite

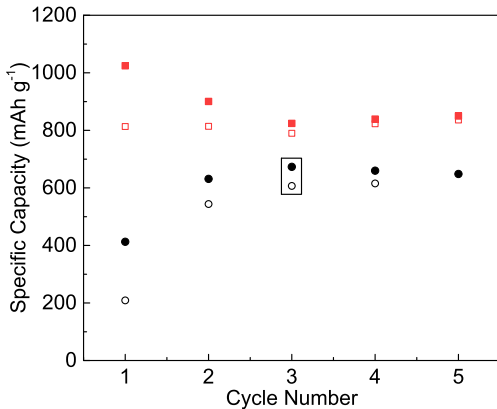
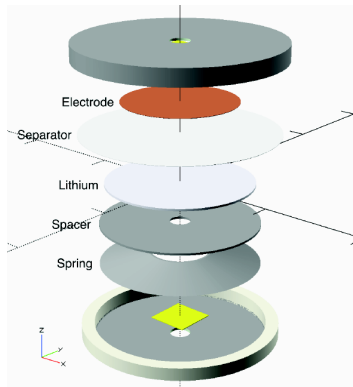
Theoretically could transfer 9 or more electrons upon lithiation



Sn<sub>4</sub>P<sub>3</sub>/graphite composite shows stable, reversible capacity of 610 mAh/g for 100 cycles at C/2 compared to rapidly fading pure Sn<sub>4</sub>P<sub>3</sub> material.

How does the lithiation process differ from that of Sn metal?

# In situ EXAFS of $\text{Sn}_4\text{P}_3$ /graphite

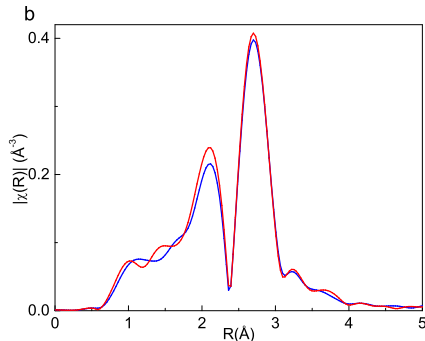
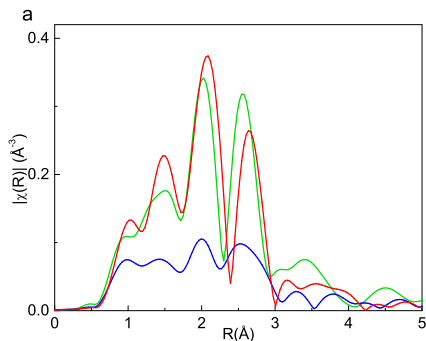


Results for *in situ* coin cell are close to the capacity of the unmodified cell at C/4, indicating good reversibility by the 3<sup>rd</sup> cycle.

# Third cycle comparison



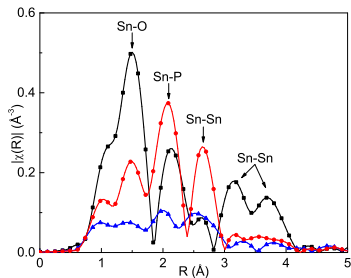
By the **third lithiation** and **third delithiation**, the difference between pure  $\text{Sn}_4\text{P}_3$  and the  $\text{Sn}_4\text{P}_3$ /graphite composite is clear.



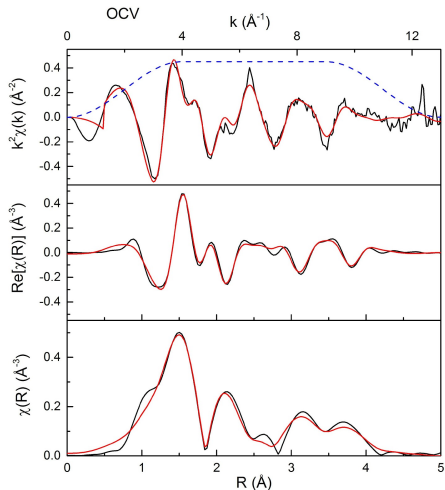
Even at the **100<sup>th</sup> delithiation**, the  $\text{Sn}_4\text{P}_3$ /graphite composite measured *ex situ* is showing the same features as at the 3<sup>rd</sup> cycle.



# Example fits

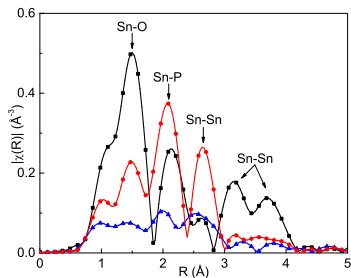


The EXAFS modeling of the  $\text{Sn}_4\text{P}_3$ /graphite electrode at OCV, 3<sup>rd</sup> lithiation, and 3<sup>rd</sup> delithiation, provides bond distances and coordination numbers

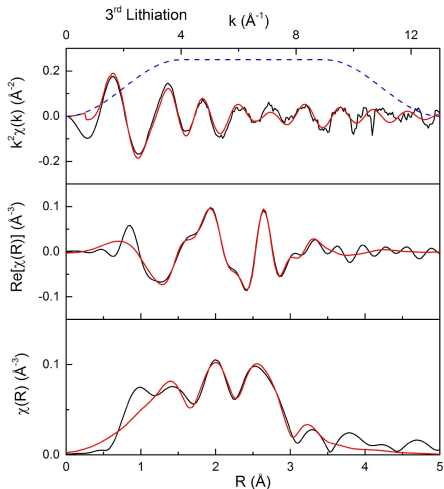


The Sn-O peak in the OCV spectrum is primarily due to the ball milling process which inevitably introduces some oxygen.

# Example fits

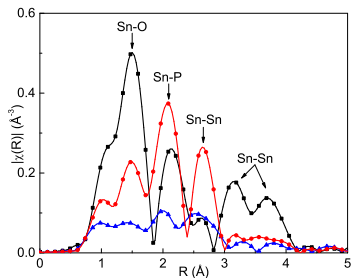


The EXAFS modeling of the  $\text{Sn}_4\text{P}_3$ /graphite electrode at OCV, 3<sup>rd</sup> lithiation, and 3<sup>rd</sup> delithiation, provides bond distances and coordination numbers



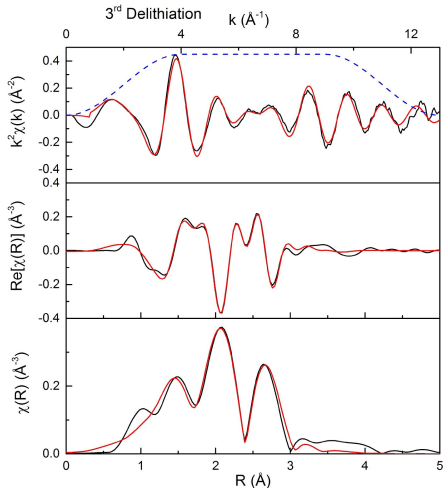
By the 3<sup>rd</sup> fully lithiated state, the EXAFS is dominated by the Sn-Li paths at 2.7  $\text{\AA}$  and 3.0  $\text{\AA}$ .

# Example fits

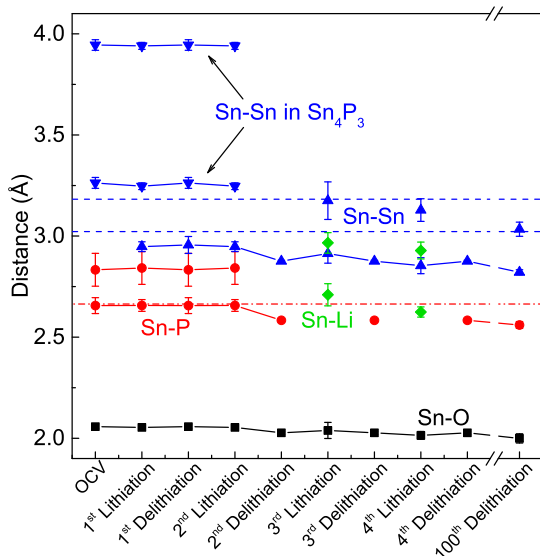


The EXAFS modeling of the  $\text{Sn}_4\text{P}_3$ /graphite electrode at OCV, 3<sup>rd</sup> lithiation, and 3<sup>rd</sup> delithiation, provides bond distances and coordination numbers

At the 3<sup>rd</sup> delithiation, the Sn-P path reappears but at a shorter distance, in an amorphous  $\text{SnP}_x$  phase.



# Sn<sub>4</sub>P<sub>3</sub>/graphite path lengths



Sn-Sn distance close to those of metallic Sn indicate the presence of small Sn clusters which may never fully lithiate

Longer Sn-P distance characteristic of Sn<sub>4</sub>P<sub>3</sub> is gone after initial conversion to the SnP<sub>x</sub> amorphous phase is complete

Only 2 Sn-Li paths present in this material

Sn-O distances remain constant, likely indicative of surface contamination

# Sn<sub>4</sub>P<sub>3</sub>/graphite coordination numbers



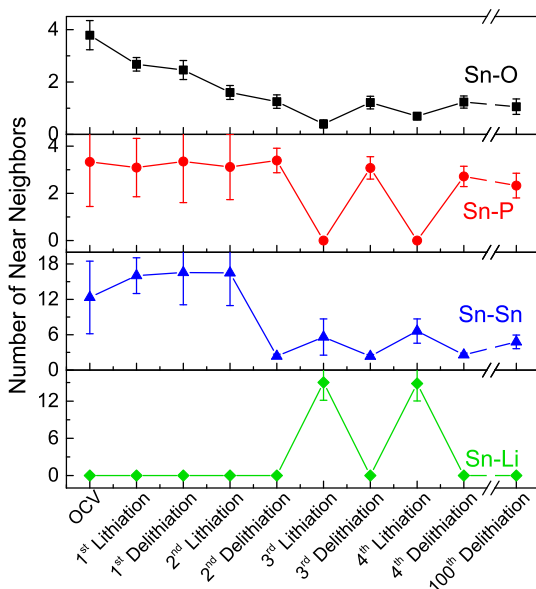
Sn-O neighbors decrease quickly, remaining small and partially reversible up to 100 cycles

Sn-P reversible after initial conversion with a slow decrease which correlates to capacity loss

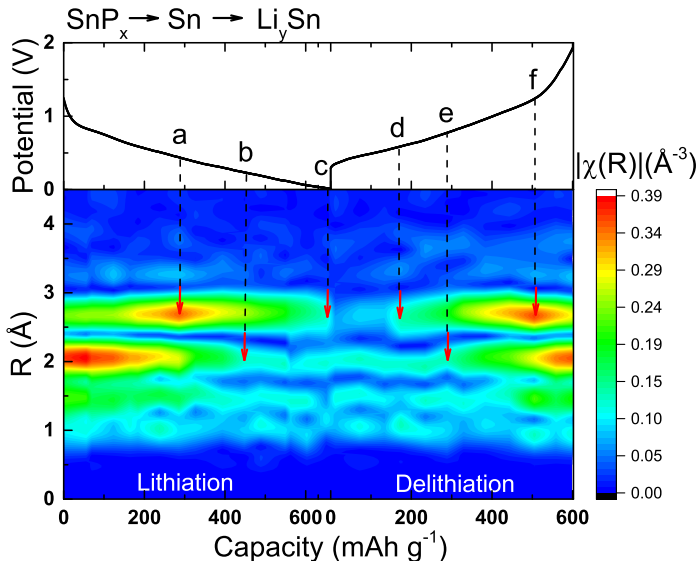
Very small Sn-Sn metallic clusters present throughout

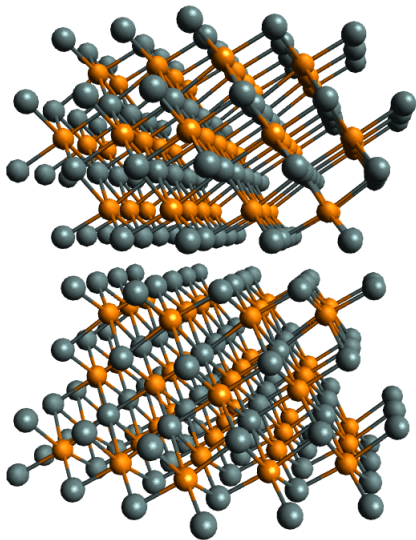
The ~3.3 Sn-P neighbors in the delithiated state indicate a possibly tetrahedral Sn coordination in SnP<sub>x</sub>

15 Sn-Li neighbors correspond to nearly full lithiation and fade with capacity.



# Third cycle dynamic snapshot





## Graphite nanoparticle composite

- provides high electronic conductivity
- inhibits Sn nanoparticle aggregation
- promotes amorphous  $\text{SnP}_x$  formation

Reversibility of amorphous  $\text{SnP}_x$  phase and surrounding  $\text{Li}_3\text{P}$

Structure of initial  $\text{Sn}_4\text{P}_3$  material may be beneficial

Ball milled composites being tested for Sn,  $\text{SnO}_2$ , and  $\text{SnS}_2$  nanoparticles

Further improvements to the in-situ cell needed to make better *in situ* studies possible

# Principal collaborators - Thank you!



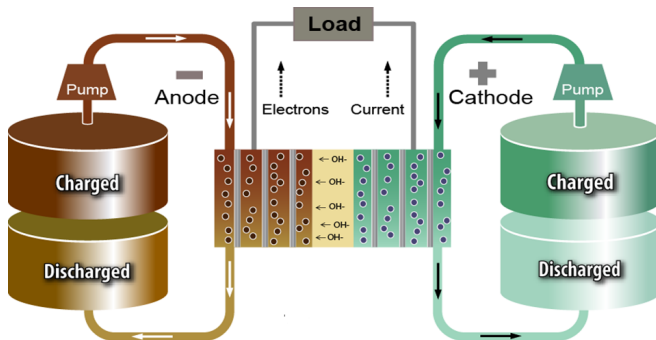
- Christopher Pelliccione – IIT Physics (Ph.D. student)
- Yujia Ding – IIT Physics (Ph.D. student)
- John Katsoudas – IIT (MRCAT staff)
- Elena Timofeeva – IIT Chemistry

Supported by

- Department of Energy ARPA-e Grant
- Department of Education GAANN Grant
- National Science Foundation MWN Grant
- Duchossois Leadership Program at Illinois Tech



# Nanoelectrofuel flow battery



Suspended electroactive nanoparticles

Advantages of flow batteries

Energy density of solid state

Chemistry agnostic

aqueous or non-aqueous

Initial ~~arpa~~ funding

IIT/Argonne collaboration

Prototype: 1 kWh total energy stored  
40 V, C/3 discharge rate

Develop commercialization plan

# Advantages of nanoelectrofuel



of active material  
in solid batteries

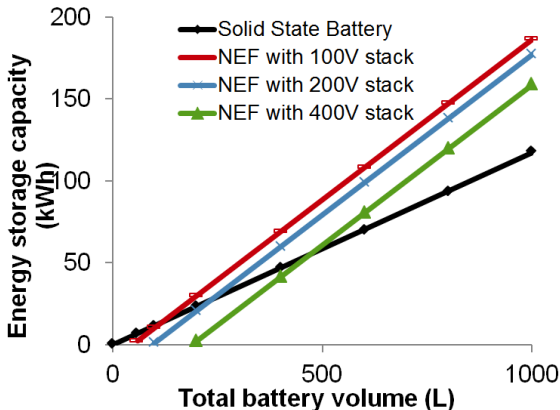


of active material  
in NEF flow batteries

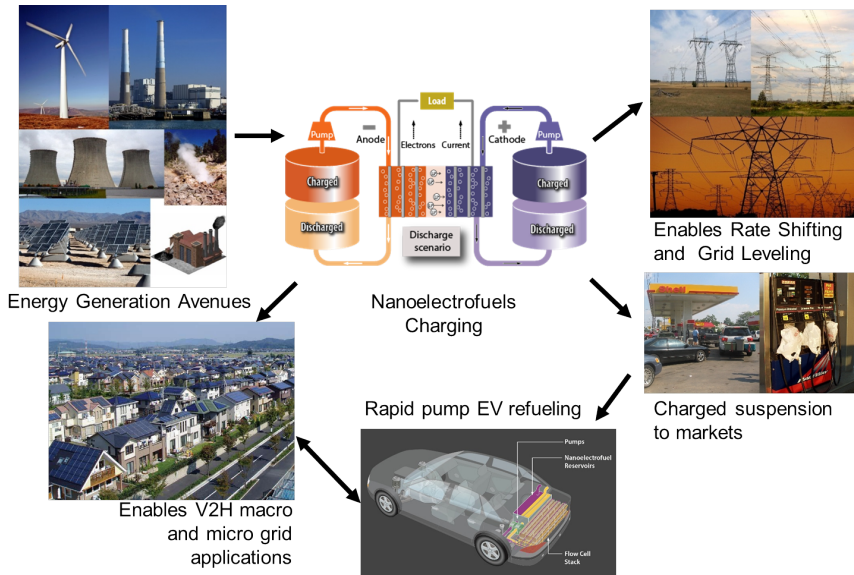
initial overhead for  
power stack depends on  
desired voltage

active material fraction  
depends on loading  
(50% shown)

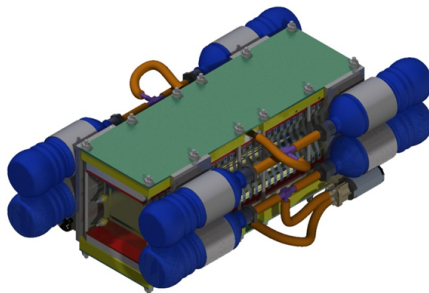
beyond 50 kWh, NEF  
has higher volumetric ca-  
pacity



# Long term vision



- What is the intrinsic performance of active materials in nanoparticle form?
- Can suspended nanoparticles be effectively charged and discharged during flow?
- How much loading can be stabilized in suspension?
- Will these nanoelectrofuels be pumpable and not destroy the enclosure materials?
- Can the technology be economical enough to compete with more established technologies?



40 V aqueous chemistry stack

25 kWh using 4.5 L of nanoelectrofuel

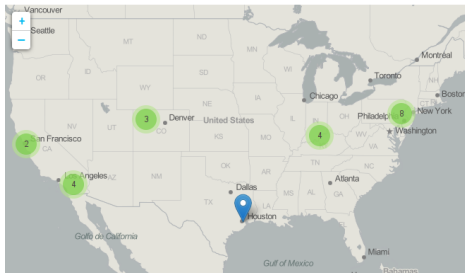
26 kg stack, 10 kg 50% loaded fluid

70 Wh/kg (compare to 40 Wh/kg for Pb-acid)

# Initial funding: the RANGE program (2014-2015)



## Robust Affordable Next Generation Energy Storage Systems



Develop transformational electro-chemical energy storage technologies for electric vehicles (EVs)

- provide greater EV driving range
- reduce overall weight of the vehicle
- maximize the overall energy stored in a vehicle
- enhance safety
- minimize manufacturing costs
- enable greater design flexibility for manufacturers

22 projects across the United States

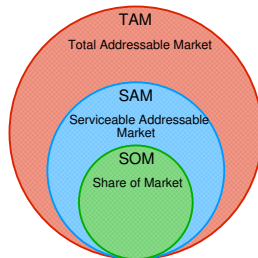
# The I-Corps experience



# The I-Corps experience



Participated in the I-Corps Energy & Transportation program sponsored by Next Energy in Detroit

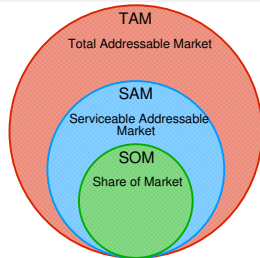


# The I-Corps experience



Participated in the I-Corps Energy & Transportation program sponsored by Next Energy in Detroit

- initial goal to grow the EV market by providing a better battery



Total Automotive Market



TAM – \$40B

SAM – \$10B

SOM – \$ 2B



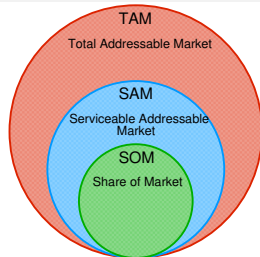


# The I-Corps experience



Participated in the I-Corps Energy & Transportation program sponsored by Next Energy in Detroit

- initial goal to grow the EV market by providing a better battery
- conducted over 60 customer interviews in 1 month



Total Automotive Market



TAM – \$40B

SAM – \$10B

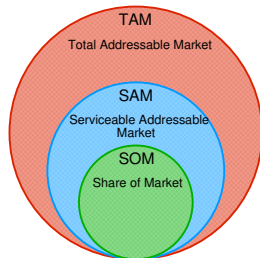
SOM – \$ 2B





Participated in the I-Corps Energy & Transportation program sponsored by Next Energy in Detroit

- initial goal to grow the EV market by providing a better battery
- conducted over 60 customer interviews in 1 month
- complex and interconnected value supply chain



Current EV Market



TAM – \$720M

SAM – \$140M

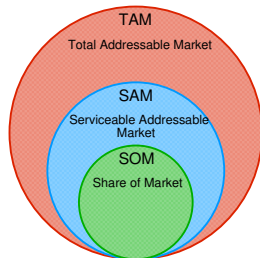
SOM – \$ 7M





Participated in the I-Corps Energy & Transportation program sponsored by Next Energy in Detroit

- initial goal to grow the EV market by providing a better battery
- conducted over 60 customer interviews in 1 month
- complex and interconnected value supply chain
- 10-20 years to break into the automotive supply chain!



Current EV Market



TAM – \$720M

SAM – \$140M

SOM – \$ 7M





Electric utility vehicles (EUVs) can bridge the “valley of death”

Participated in the I-Corps Energy & Transportation program sponsored by Next Energy in Detroit

- initial goal to grow the EV market by providing a better battery
- conducted over 60 customer interviews in 1 month
- complex and interconnected value supply chain
- 10-20 years to break into the automotive supply chain!

Current EUV Market



TAM – \$600M

SAM – \$300M

SOM – \$ 75M





Participated in the I-Corps Energy & Transportation program sponsored by Next Energy in Detroit

- initial goal to grow the EV market by providing a better battery
- conducted over 60 customer interviews in 1 month
- complex and interconnected value supply chain
- 10-20 years to break into the automotive supply chain!

Electric utility vehicles (EUVs) can bridge the “valley of death”

- EUV market 5× larger than EV

Current EUV Market



TAM – \$600M

SAM – \$300M

SOM – \$ 75M





Participated in the I-Corps Energy & Transportation program sponsored by Next Energy in Detroit

- initial goal to grow the EV market by providing a better battery
- conducted over 60 customer interviews in 1 month
- complex and interconnected value supply chain
- 10-20 years to break into the automotive supply chain!

Electric utility vehicles (EUVs) can bridge the “valley of death”

- EUV market 5× larger than EV
- simpler vehicles with smaller value supply chain

Current EUV Market



TAM – \$600M

SAM – \$300M

SOM – \$ 75M





Participated in the I-Corps Energy & Transportation program sponsored by Next Energy in Detroit

- initial goal to grow the EV market by providing a better battery
- conducted over 60 customer interviews in 1 month
- complex and interconnected value supply chain
- 10-20 years to break into the automotive supply chain!

Electric utility vehicles (EUVs) can bridge the “valley of death”

- EUV market 5× larger than EV
- simpler vehicles with smaller value supply chain
- lead-acid batteries must be replaced every year

Current EUV Market



TAM – \$600M

SAM – \$300M

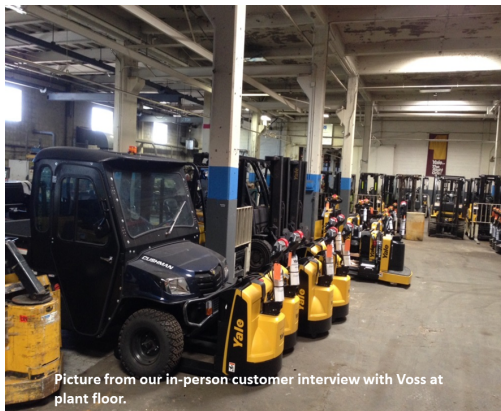
SOM – \$ 75M



# The first product



EUVs and fork lifts are  
already predominantly  
electric



Picture from our in-person customer interview with Voss at plant floor.



# The first product

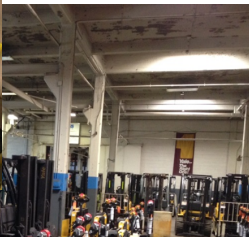


Picture from our in-person customer interview with Voss at plant floor.

EUVs and fork lifts are already predominantly electric

batteries replaced at factory each year

# The first product



EUVs and fork lifts are  
already predominantly  
electric

batteries replaced at fac-  
tory each year

typical motor is 36-40V

# The first product



EUVs and fork lifts are already predominantly electric

batteries replaced at factory each year

typical motor is 36-40V

4-pack of lead-acid batteries are most common

# The first product



EUVs and fork lifts are already predominantly electric

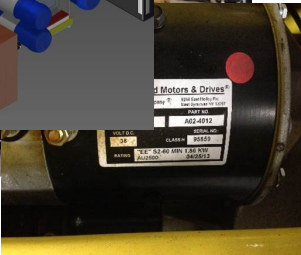
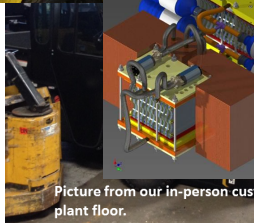
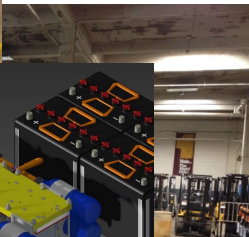
batteries replaced at factory each year

typical motor is 36-40V

4-pack of lead-acid batteries are most common

12-hour charge cycle required between uses

# The first product



EUVs and fork lifts are already predominantly electric

batteries replaced at factory each year

typical motor is 36-40V

4-pack of lead-acid batteries are most common

12-hour charge cycle required between uses

a perfect match for our nanoelectrofuel prototype battery



THE COMPANY FOR LIQUID BATTERIES

[Home](#) [About](#) [Technology](#) [Influit Info](#) [Contact](#) [FAQ](#)

## Renewable and Sustainable Liquid Energy

[DISCOVER MORE](#)

***Using nanotechnology to accelerate society's transition to  
sustainable energy future***